Numerical simulation and advanced thermo-mechanical characterization of additively manufactured PEEK 3D-auxetic structures

C Solek[1,*], J Crespo-Sánchez[1], S Fuentes del Toro[2], J Ayllón[1], A M. Camacho[1], J Rodríguez-Hernández[3], A Rodríguez-Prieto[1]

[1] Department of Manufacturing Engineering, UNED, (Madrid – Spain); *csolek@ind.uned.es
[2] Department of Mechanical Engineering, UC3M, (Madrid – Spain)
[3] Institute of Polymer Science and Technology (ICTP-CSIC), (Madrid-Spain)

OBJECTIVES

PEEK is a high-performance semi-crystalline polymer with outstanding mechanical, thermal and chemical properties, making it increasingly attractive for additive manufacturing (AM) of auxetic structures due to its high energy absorption, damping behaviour and lightweight potential (Figure 1) [1,2]. However, process-induced thermal gradients, crystallization phenomena and anisotropic behaviour generate residual stresses and distortions that compromise the dimensional accuracy and performance of these structures.

To address this challenge, a comprehensive thermo-mechanical characterization of PEEK was conducted combining Dynamic Mechanical Analysis (DMA), Digital Image Correlation (DIC) and Differential Scanning Calorimetry (DSC) to determine the coefficient of thermal expansion (CTE) and crystallization kinetics. The experimentally identified parameters were subsequently implemented in Digimat® to model the material behaviour and simulate the FFF manufacturing process, enabling the anticipation of process-induced defects and the virtual assessment of component performance prior to fabrication.

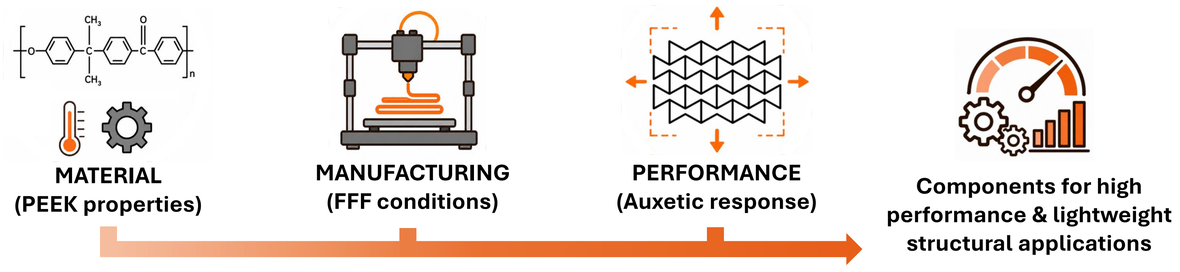

Figure 1. PEEK as a high-performance engineering polymer for additively manufactured auxetic structures, combining lightweight design, energy absorption and damping capabilities.

METHODOLOGY

1) DMA-DIC Based CTE Determination

The CTE was determined using a DMA-DIC. A temperature ramp from 20 °C to 315 °C was applied under a constant load of 100 mN, while longitudinal strain was continuously monitored from the acquired images.

To validate the proposed methodology, measurements were first performed on aluminium and Grade 2 titanium reference specimens (Figure 2). The CTE was calculated from the relative longitudinal strain measured by DMA-DIC (Eq. 1). The method was considered valid when the experimental CTE values differed by less than 10% from literature values and exhibited coefficients of variation below 5% (Table 1).

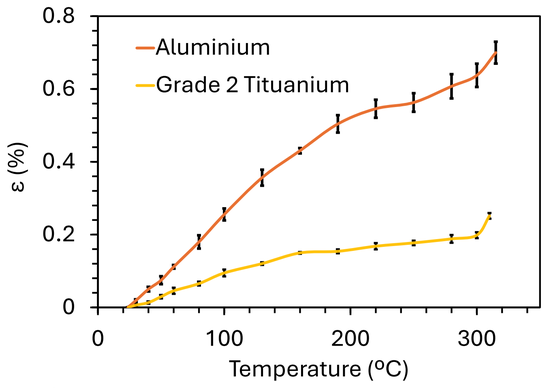

Figure 2. Relative longitudinal strain versus temperature for Al and Grade 2 Ti reference specimens.

$$Eq.1: \quad \alpha_r = \frac{\varepsilon/100}{\Delta T}$$

α_r : CTE of the reference (°C^{-1})
ε : relative longitudinal strain (%)
ΔT: temperature change (°C)

	$\alpha_{literature}$ (°C^{-1})	α_r (°C^{-1})	CV (%)
Al	$2.23 \cdot 10^{-5}$	$2.4 \cdot 10^{-5} \pm 0.1 \cdot 10^{-5}$	4.08
Grade 2 Ti	$8.4 \cdot 10^{-6}$	$8.7 \cdot 10^{-6} \pm 0.2 \cdot 10^{-6}$	2.60

Table 1. Experimental and literature [3] CTE values for the reference materials, together standard deviation and coefficient of variation (CV).

After validation, the same experimental procedure was applied to commercial Z-PEEK filament and FFF-manufactured specimens printed at 0° and 45° orientations. The measured strain-temperature curves were used to evaluate the influence of printing orientation on thermal expansion behaviour (Figure 3).

No significant differences were observed between the analyzed configurations, indicating a negligible influence of printing orientation on the CTE of the studied material (Figure 3). The final CTE value (Table 2) was calculated (Eq. 2) using the Grade 2 titanium reference and subsequently implemented in the Digimat® material model.

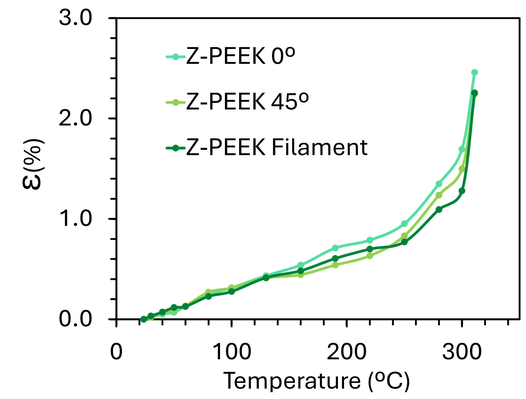

Figure 3. Relative longitudinal strain as a function of temperature for Z-PEEK specimens printed at 0° and 45°, together with the commercial filament.

$$Eq.2: \quad \alpha_m = \frac{\Delta L_m - \Delta L_r}{\Delta T \cdot L_0} + \alpha_r$$

ΔL_m : length variation of the specimen (m)
ΔL_r: length variation of the reference (m)
L_0: initial specimen length (m)
α_m : CTE of the specimen (°C^{-1})
α_r : CTE of the reference (°C^{-1})
ΔT : temperature change (°C)

	$\alpha_{literature}$ (°C^{-1})	α_m (°C^{-1})
Z-PEEK	$13.0 \cdot 10^{-5}$ *	$9.1 \cdot 10^{-5} \pm 0.2 \cdot 10^{-5}$

Table 2. Experimental and literature [4] CTE values for Z-PEEK, including the corresponding standard deviation. * The literature value corresponds to a different PEEK supplier, explaining the observed discrepancy.

3) Digimat® Simulation

The experimentally determined material properties were implemented in finite element (FE) simulation, and the resulting material model was transferred to Digimat-AM to simulate the FFF manufacturing of a PEEK re-entrant auxetic structure (Figure 6). A parametric study was conducted by varying the chamber and extrusion temperatures (Table 4) [5]. All other process parameters were kept constant: bead width (0.5 mm), layer height (0.25 mm), draw speed (60 mm/s), convection coefficient (0.015 mW/(mm^2·°C)), room and final temperature (23 °C).

Simulation	Extrusion Temp. (°C)	Chamber Temp. (°C)
S1	400	100
S2	400	125
S3	400	150
S4	400	170
S5	400	200
S6	375	200
S7	425	200
S8	450	200

Table 4. Digimat® simulation matrix for the parametric study.

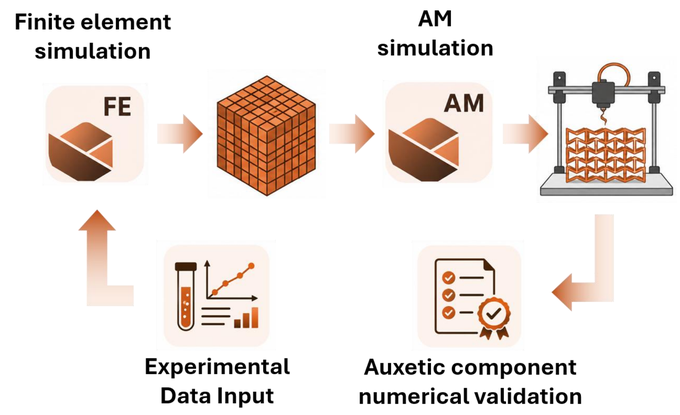

Figure 6. Digimat® workflow from material characterization to auxetic component validation.

2) DSC Based Crystallization Kinetics Determination

The non-isothermal crystallization behaviour of Z-PEEK was characterized by DSC at cooling rates of 1, 2, 5, 10, 15 and 20 °C/min (Figure 4).

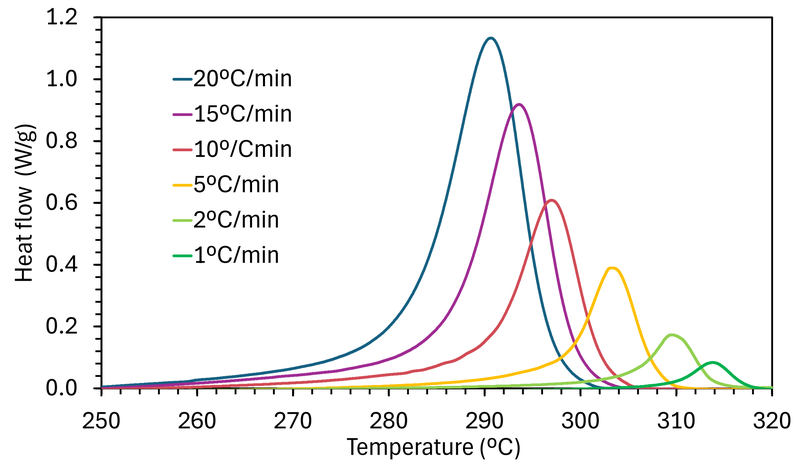

Figure 4. DSC characterization of Z-PEEK at different cooling rates.

Relative crystallinity (X_{rel}) was calculated from the crystallization exotherms and used to calibrate a Nakamura model coupled with Hoffman-Lauritzen theory (Eq. 3-4), where the temperature-dependent crystallization rate $K(T)$ is governed by the Hoffman-Lauritzen formulation. The equilibrium melting temperature (T_{m0} = 395 °C), the activation energy for molecular transport (U^* = 6270 J/mol), the limiting temperature for molecular mobility (T_∞ = 113 °C), and the universal gas constant (R = 8.314 Jmol^{-1}K^{-1}) were fixed according to literature values. The pre-exponential factor (K_0) and the nucleation parameter (K_g) were determined through nonlinear least-squares fitting.

$$Eq.3: \quad X(t) = 1 - \exp\left[-\left(\int_0^t K(T)\,dt\right)^n\right]$$

$$Eq.4: \quad K(T) = K_0 \exp\left[-\frac{U^*}{R(T - T_\infty)}\right] \exp\left[-\frac{K_g}{T(T_{m0} - T)f}\right]$$

To identify the most representative crystallization mechanism, the Avrami exponent (n) was selected based on the lowest fitting error (RMSE) (Table 3).

n	K_0 (s^{-1})	K_g (K^2)	$RMSE$
1	**6.16×10^5**	**7.15×10^5**	**0.0847**
2	2.03×10^5	6.48×10^5	0.1107
3	2.03×10^5	6.43×10^5	0.1266

Table 3. Values of K_0, K_g and RMSE obtained from the nonlinear fitting procedure for each Avrami exponent (n).

The lowest fitting error was obtained for n = 1, indicating that the crystallization behaviour of the studied PEEK can be accurately represented using a first-order nucleation-growth kinetic model (Figure 5). Therefore, the corresponding parameters were selected for implementation in the Digimat® material model.

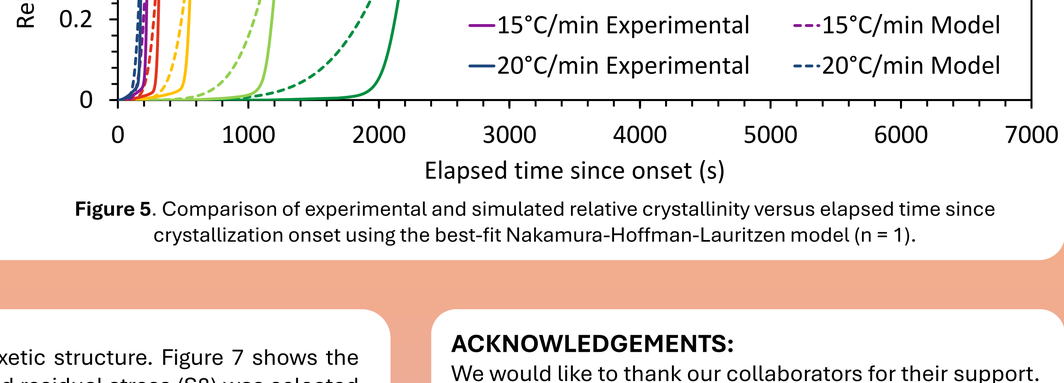

Figure 5. Comparison of experimental and simulated relative crystallinity versus elapsed time since crystallization onset using the best-fit Nakamura-Hoffman-Lauritzen model (n = 1).

RESULTS & CONCLUSIONS

Chamber temperature was found to have a greater influence than extrusion temperature on both warpage and internal stress in the auxetic structure. Figure 7 shows the maximum warpage and Von Mises stress for all simulated printing conditions in Digimat-AM. The configuration with the lowest warpage and residual stress (S8) was selected as optimal, with detailed results presented in Figure 8. These results demonstrate that Digimat-AM, combined with experimental material data, enables numerical validation of the manufactured components, provides a reliable predictive framework for identifying the key process parameters affecting final part quality.

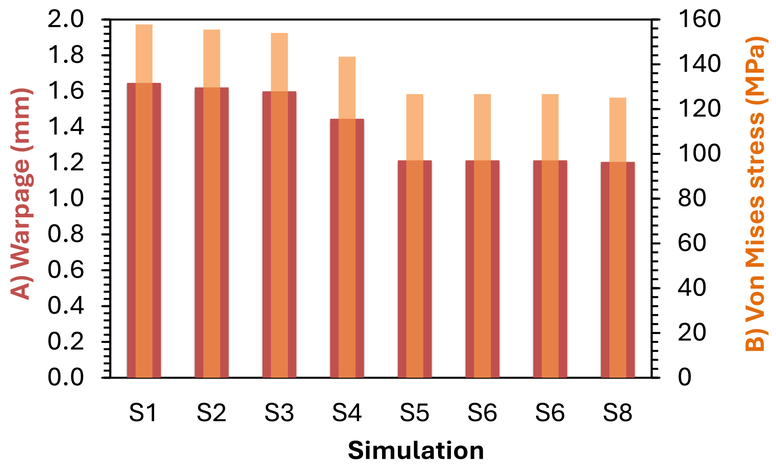

Figure 7. A) Warpage and B) Von Mises stress for the simulated printing conditions in Digimat-AM.

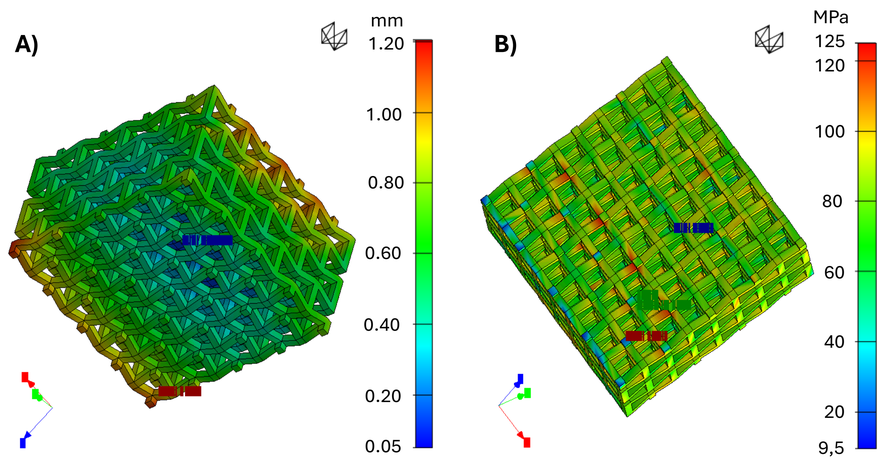

Figure 8. A) Warpage and B) Von Mises stress distribution for the optimal configuration S8: chamber temperature 200 °C, extrusion temperature 450 °C.

ACKNOWLEDGEMENTS:

We would like to thank our collaborators for their support. This research was conducted within the framework of the UNED Doctorate Program in Industrial Technologies and funded by projects PID2022-143329OA-I00 and PID2023-151687OB-I00, with additional support from PIT FAB3D, PTI + Salud Global, and PTI + SUSPLAST (CSIC).

REFERENCES:

1. Ren, X., Das, R., Tran, P., Ngo, T. D., Xie, Y. M., *Smart Materials and Structures*, 27 (2018) 023001
2. Dua, R., Rashad, Z., Spears, J., Dunn, G., Maxwell, M., *Polymers*, 13 (2021) 4046
3. Corruccini, R. J., Gniewek, J. J., *Thermal Expansion of Technical Solids at Low Temperatures*, 29 (1961).
4. Mitsubishi Chemical Advanced Materials, *Ketron™ 1000 PEEK: Product Datasheet* (2024).
5. Crespo-Sánchez, J., Fernández, D., Solek, C., Ayllón, J., Fuentes del Toro, S., Camacho, A. M., Rodríguez-Prieto, Á., Polymers, 18 (2026) 1468.